J Nanopart Res (2015) 17:70
DOI 10.1007/s11051-015-2876-x

RESEARCH PAPER

Polystyrene nanoparticles affect *Xenopus laevis* development

Margherita Tussellino · Raffaele Ronca · Fabio Formiggini · Nadia De Marco · Sabato Fusco · Paolo Antonio Netti · Rosa Carotenuto

Received: 24 April 2014 / Accepted: 16 January 2015 / Published online: 4 February 2015

Abstract Exposing living organisms to nanoparticulates is potentially hazardous, in particular when it takes place during embryogenesis. In this investigation, we have studied the effects of 50-nm-uncoated polystyrene nanoparticles (PSNPs) as a model to investigate the suitability of their possible future employments. We have used the standardized Frog Embryo Teratogenesis Assay-*Xenopus* test during the early stages of larval development of *Xenopus laevis,* and we have employed either contact exposure or microinjections. We found that the embryos mortality rate is dose dependent and that the survived embryos showed high percentage of malformations. They display disorders in pigmentation distribution, malformations of the head, gut and tail, edema in the anterior ventral region, and a shorter body length compared with sibling untreated embryos. Moreover, these embryos grow more slowly than the untreated embryos. Expressions of the mesoderm markers, *bra* (T-box *Brachyury* gene), *myod1* (myogenic differentiation1), and of neural crest marker *sox9* (sex SRY (determining region Y-box 9) transcription factor *sox9*), are modified. Confocal microscopy showed that the nanoparticles are localized in the cytoplasm, in the nucleus, and in the periphery of the digestive gut cells. Our data suggest that PSNPs are toxic and show a potential teratogenic effect for *Xenopus* larvae. We hypothesize that these effects may be due either to the amount of NPs that penetrate into the cells and/or to the "corona" effect caused by the interaction of PSNPs with cytoplasm components. The three endpoints of our study, i.e., mortality, malformations, and growth inhibition, suggest that the tests we used may be a powerful and flexible bioassay in evaluating pollutants in aquatic embryos.

Keywords Embryogenesis · Teratogenic · Nanoparticles · Gene expression · Toxicity

Electronic supplementary material The online version of this article (doi:10.1007/s11051-015-2876-x) contains supplementary material, which is available to authorized users.

M. Tussellino · R. Ronca · N. D. Marco · R. Carotenuto (✉)
Department of Biology, University of Naples Federico II, Naples, Italy
e-mail: rosa.carotenuto@unina.it

F. Formiggini · S. Fusco · P. A. Netti
Center for Advanced Biomaterials for Health Care (IIT@CRIB), Italian Institute of Technology, Naples, Italy

Introduction

Nanomaterials (NMs) are used in a variety of applications, including cosmetics and personal care products, electronics, drug delivery systems, medical diagnostics, manufacturing technologies, and paints. In particular, in medicine, nanoparticles (NPs) offer a unique opportunity to overcome physiological barriers

and deliver bioactive agents to specific cells and targets (Guarnieri et al. 2011; 2013; Kumar et al. 2012). However, the use of NMs is a threat because of their potential toxic effects on living organisms (Kumar et al. 2012). Therefore, an increasing effort of the research community has recently been devoted to manage the sustainability of NPs employment in biology. Experimental evidence shows that NPs may enter the environment and be associated with the increased risk of certain diseases in living organisms (Bacchetta et al. 2012; Casado et al. 2013; Kumar 2006), including humans (Kumar et al. 2012). In particular, it is well known that aquatic environments are at risk of exposure to pollutants, as they represent a sink for most environmental contaminants (Krysanov et al. 2010; Scown et al. 2010; Casado et al. 2013). This new form of pollution, known as nanotoxicity, introduces a serious problem to the scientific community. The relative novelty of the subject, the complexity of the interaction occurring between NMs and living systems, and the lack of history or methods (Kahru and Dubourguier 2010; Kumar et al. 2012), make it difficult to provide standardized measurements of the toxicity level of the new nanotechnology industry products. NPs have the same chemical composition of the bulk, yet have different toxicological properties according to size, shape, and surface covering. Dose, route of administration, and exposure as well are critical factors that affect the degree of toxicity produced by any particular type of NP. It is for this reason that a careful and rigorous toxicity testing is necessary before any NP is declared to be safe for broad use (Sanfins et al. 2014; Kumar et al. 2012). In particular, polystyrene is one of the most heavily used polymers in routine daily activity and is a potential strong pollutant of aquatic environment. Among its many applications, it is commonly used as a food container and carrier. In nanomedicine and nanotechnology, understanding the potential consequences of employing nanoscale materials in various applications, especially in embryology and biomedical field, is critically an important procedure for the protection of the general public.

Liu et al. (2011) showed that uncoated PSNPs are generally inert and nontoxic, when negatively charged. However, Hardy et al. (2013), investigating comparatively the immunological imprints of uncoated polystyrene nanoparticles (PSNPs) 50 nm (PS50G) and 500 nm (PS500G), found that these particles imprint a differentially modulated induction of acute allergic airways inflammation, with PS50G but not PS500G significantly inhibiting adaptive allergen-specific immunity. These effects are not limited to the respiratory system, as increases in acute cardiovascular events were also observed (Enright et al. 2013). During mouse embryogenesis, fluorescent polystyrene particles were employed, as an efficient and safe tracking method to examine the roles of particles size and surface modification in particles translocation, by Tian et al. (2009). Yet, under this condition, growth inhibition was observed in embryos containing those nanoparticles. Mouse embryos derived from mother exposed to mixed-size PSNPs did not show inhibition of embryo development at the blastocyst stage, although they were internalized, suggesting a lack of embryotoxicity (Bosnam et al. 2005). However, the observation that fluorescent PSNPs up to 240 nm were able to cross the placental barrier (Wick et al. 2010) requires further studies for screening embryotoxicity, although they do not affect the intrinsic characteristics of this organ. Although PSNPs deleterious effects were observed in aquatic species (Casado et al. 2013), such as zebrafish (Cedervall et al. 2012), the effects of PSNPs on aquatic embryos have not been investigated yet.

The aim of our work is to understand the effects that the accumulation of uncoated fluorescent 50 nm PSNPs has during the embryogenesis of the well-known and robust model *Xenopus laevis*, for the assessment of PSNPs effects in aquatic larvae, thereby contributing to the understanding of their possible toxicity and subsequent harm for general community. In *Xenopus*, reports dealing with the potential effects of these nanoparticles are not available. *X. laevis* is an aquatic organism development of which occurs outside the mothers body, therefore allowing monitoring anlagen morphogenesis in detail. Although the use of *X. laevis* has been hampered by its relatively long reproduction time compared with *D. melanogaster* and *C. elegans*, its large embryonic cells and the ease of manipulation in early embryogenesis continue to have remarkable research potential. *Xenopus* facilitates biophysical and physiological approaches to understand developmental signals that can be transferred to higher vertebrates, including humans (Tomlinson et al. 2005; Takagi et al. 2013). The PSNPs size range (40–60 nm) used in our work is known to represent the most efficient size for cellular uptake

(Nam et al. 2013) and were chosen as model to investigate the suitability of their possible employments in future studies such as carrier or tracking methods (Chang 2010). We have employed the range of concentration used to test these NPs in other organisms (Casado et al. 2013) and applied the Frog Embryo Teratogenesis Assay-*Xenopus* (FETAX) protocol. We assayed two procedures of administration: the dilution in culture medium (contact embryos) and microinjection in the early stage of development (one of the cells at the two cells stage). Interestingly, in microinjected embryos, the uninjected side can be considered as the natural control of each test to check if particles penetrate into the sister cell, while, in contact embryos, the penetration in adjacent cells cannot be easily tested. In contact embryos, nanoparticles, differently from the injected embryos, encounter a complex mixture of extracellular proteins in the intercellular space, which cover them and can determine their interaction with the cellular environment (Fleischer and Payne 2014; Xu et al. 2014). The three endpoints of this test, i.e., mortality, malformations, and growth inhibition, render it a powerful and flexible bioassay to evaluate pollutants in water (Dumont et al. 1983).

Materials and methods

Animals

Adult *X. laevis* were obtained from Nasco (Fort Atkinsons, Wisconsin, USA). They were kept and used at the Department of Biology of the University of Naples, Federico II, according to the guidelines and policies dictated by the University Animal Welfare Office in agreement with international rules and in strict accordance with the recommendations in the Guide for the Care and Use of Laboratory Animals of the National Institutes of Health of the Italian Ministry of Health. The protocol was approved by the Committee on the Ethics of Animal Experiments (Centro Servizi Veterinari) of the University of Naples Federico II (Permit Number: 2014/0017970). All procedures were performed according to Italian ministerial authorization (DL 116/92) and European regulations on the protection of animals employed for experimental and other scientific purposes. All surgical procedures were performed under ethyl 3-aminobenzoate methanesulfonate (Sigma). All trials were adopted to minimize suffering. To obtain eggs, *X. laevis* females were injected in the dorsal lymphatic sac with 500 units of Gonase (AMSA) in amphibian Ringer solution (111 mM NaCl, 1.3 mM $CaCl_2$, 2 mM KCl, 0.8 mM $MgSO_4$, in 25 mM Hepes, pH 7.8). Fertilized eggs and embryos were obtained by standard insemination methods and staged according to Nieuwkoop and Faber (1956).

PSNPs characterization

Red fluorescent, unmodified polystyrene NPs with diameters of about 50 nm were purchased from Duke Scientific Corporation. Composition: Polystyrene. Dyes: Firefly fluorescent red (542/612 nm). Density: 1.05 g/cm^3 (1.5×10^{14}NPs/ml). Index of Refraction: 1.59 at 589 nm (25 °C). Dynamic light scattering (DLS), made with a Zetasizer Nano-ZS (Malvern Instruments, Worcestershire, UK), was performed to measure PSNPs size and z-potential. Measurements were conducted at 25 and 18 °C, with or without sonication. We performed the DLS on amphibian solutions, 10 % Ringer pH 6.5 or FETAX pH 7.4 (106 mM NaCl, 11 mM $NaHCO_3$, 4 mM KCl, 1 mM $CaCl_2$, 4 mM $CaSO_4$, 3 mM $MgSO_4$) or in H_2O, containing the PSNPs at three different concentrations: 4.5, 9, and 18 mg/L. We made these tests both in the absence and in the presence of embryos (18° C, the breeding temperature). Each measurement was repeated five times, and all the measurements were done in triplicate. The measurements were carried out in agreement with the embryonic stages evaluated for mortality data. i.e., stages: 10, 14, 28, 46, corresponding to days: 1, 2, 4, and 7 post-fertilization, respectively.

PSNPs exposition and microinjections

Stages 2 embryos were placed and grown in 10 % Ringer or FETAX solution containing PSNPs at the following concentrations: 4.5, 9, or 18 mg/L. FETAX can be used to test single compounds (Bantle and Dawson 1988). All embryos were harvested until stage 45/46. At stage 40/41, *X. laevis* embryos opened their mouth (Nieuwkoop and Faber 1956), and ingestion became the main route of PSNPs intake. Since in the following days the grazing behavior of the larvae became very active, the number of ingested particles increased. The embryos survival and phenotype were

checked daily. All experiments were carried out at about 18 °C in triplicate. As control, sibling embryos were used. The mortality percentage was calculated on the number of dead embryos versus their total number at the beginning of the test. Dose-dependent correlation between PSNPs concentration and embryos mortality rates was also analyzed. The relationship between the control and the treated groups, along with the percentage of dead embryos and the observed malformations, was investigated with Chi square test, using the Yate's correction for continuity or Fisher's Exact test. To evaluate differences in growth retardation among groups, the ANOVA with nonparametric Kruskal-Wallis test and Dunns test for post hoc analysis was used to compare all pairs of columns. The survival distributions in control and experimental groups were also assessed in terms of significance using nonparametric Mantel-Cox test. For all statistical tests, we employed the Graph Pad Prism 5 software (San Diego, California USA). The methods utilized here are comparable to those of other authors who have investigated the NPs on aquatic organism (Kahru and Dubourguier 2010; Krysanov et al. 2010; Bacchetta et al. 2012; Pompa et al. 2010). Alternatively, the PSNPs were microinjected into embryos using a Drummond 'Nanoject II'. The nanoparticle solutions were injected into the animal hemisphere of a single cell of two-cell stage embryos. After injection, embryos were kept in 3 % Ficoll (Fisher Bioreagent)/10 % Ringer at about 18 °C. The maximum volume we could inject was 4.6 nL. The concentrations of the solutions were the same as those utilized for contact experiments. The solutions of microinjections contain 1.38×10^6 (0.08 ng) or 0.69×10^6 (0.04 ng) or 0.345×10^6 (0.02 ng) PSNPs diluted in phenol red (vital dye) and 300 pg of pCS2MTGFP mRNA coding for GFP (Green Fluorescent Protein). GFP was always co-injected to label the injected side. Capped synthetic RNAs were generated by in vitro transcription using the Sp6 Message Machine kit (Ambion, Austin, TX, USA). As control, GFP-injected and -uninjected sibling embryos were utilized. The phenotypes of the injected embryos were scored when embryos reached stage 11, 11.5, 13, 19, 25, 28, 35, or 45/46, corresponding to the known stages of anlagen morphogenesis. All the samples were photographed using a Leica MZ16F UV stereomicroscope, equipped with a Leica DFC 300Fx camera and IM50 Image Manager Software.

Whole mount in situ hybridization

Wild-type *X. laevis* embryos, or embryos injected in one blastomere at stage 2 with PSNPs diluted in phenol red, were fixed in MEMFA (MOPS (4-morpholinepropanesulfonic acid) EGTA $MgSO_4$ FormAldehyde) (100 mM MOPS pH 7.4, 2 mM EGTA, 1 mM $MgSO_4$ 3.7 % v/v Formaldehyde) (see Gont et al. 1993) at stage 11, 11.5, 13, 19, 25, and 45/46 and stored in 100 % ethanol at -20 °C. In situ hybridizations (see Vaccaro et al. 2006) were performed with antisense digoxigenin-labeled RNA of *bra,* or *myod1*, or *sox9* synthesized with SP6 polymerase (Roche, Mannheim, Germany). In situ hybridizations with antisense *sox9* RNA were also performed on embryos exposed to PSNPs diluted 18 mg/L and fixed in MEMFA at stage 46. All hybridized embryos were photographed using a Leica MZ16F equipped with a Leica DFC 300Fx camera and IM50 Image Manager Software. *myod1,* and *sox9* probes are a kind gift from Dr M. Ori, University of Pisa, Italy.

Cloning of fragment *bra* for in situ hybridization

For total RNA extraction, embryos at stage 19 were homogenized using Tri-Reagent (Sigma) according to the supplier instructions. cDNA synthesis was performed using SuperScriptVILO cDNA Syntesis Kit (Invitrogen). The partial coding DNA of *bra* (880 bp) was obtained by PCR, using the primers forward: 5′-tcacccagactcacccaactt-3′ and reverse: 5′-gtgccgtgacatcatactgg-3′, on the basis of the *X. laevis* sequence of the *brachyury* (T) gene (X*bra*), (GenBank: M77243.1). The PCR products were cloned into the pCR2 vector (TA Cloning Dual Promoter, Life Technologies, Carlsbad, CA, USA). The product was purified using the miniprep High Pure Plasmid Isolation Kit (Roche, Mannheim; Germany). pCR2-*bra* was digested with Not1 (Roche) and purified using PureLink PCR Purification Kit. Riboprobes were transcribed with Sp6 polymerase using RNA labeling (SP6/T7) kit (Roche) and purified with mini Quick Spin Columns (Roche).

Histology

Embryos were fixed at stage 46 in 4 % formaldehyde at 4 °C and stored in 100 % methanol at −20 °C. Frozen sections of 7 μm thickness were obtained after

embedding and freezing in Killik (Bio Optica, Milan, Italy). Nuclei were counter-stained with DAPI (4′,6-Diamidino-2-Phenylindole,Dihydrochloride, SIGMA) (1:1,000 in 100 % ethanol). Sections were observed and photographed using a Leica CTR 6500 UV microscope equipped with a Leica Application Suite.

Confocal microscopy

Embryos were fixed at stage 46 in MEMFA and then 60-µm-thick sections were obtained after embedding and freezing in Killik (Bio Optica Milan, Italy). Intestinal sections prepared for observation under the confocal microscope were incubated with WGA-FITC conjugates (Wheat Germ Agglutinin-Fluorescein Iso-ThioCyanate, Molecular probes), a kind gift from Dr D. Guarnieri (CRIB, Naples, Italy), diluted 1:200 in PBS containing 0.5 % BSA and 0.1 % Triton X100 for 1 h at RT. The WGA excess was eliminated by several washes in PBS.

Sections were observed and photographed using a Leica SP5 confocal laser scanning microscope. An Ar laser was used to produce the excitation laser line at 488 nm, and a HeNe laser was used to produce the excitation laser line at 543 nm. Fluorescence emission wavelength-bands were 500–530 nm for green fluorescence (488 nm excitation) and 560–650 nm for red fluorescence (543 nm excitation). Image acquisition was standardized maintaining laser power, photomultiplier, pinhole aperture, and confocal scanner settings constant for all experiments. Sections were spaced at 0.7 µm intervals, and 25 × 0.95 a HCX IRAPO L 25 × 0.95 W 0.17 water immersion objective was utilized. For each sample, a total number of 80 optical sections (1.4 µm thick) were analyzed. Images were processed by LAS AF confocal software.

Results

PSNPs characterization

To elucidate the colloidal stability of nanoparticles, we carried out measurements of the z-potential. It was reported that the colloidal stability of NPs in suspension is strongly pH-dependent, mainly due to electrostatic repulsion. The PSNPs z-potentials measured on Ringer, FETAX and in water, within 1 h from dilution at the concentrations of 9 and 18 mg/L are about 30 mV, indicating that PSNPs do not form aggregates in the solutions we utilized (Table S1). This is in agreement with data in the literature reporting that, at z-potential values of ±30 mV, electrostatic interactions between particles are strong enough for electrostatic stability, while at intermediate values, near their isoelectric point, particles can flocculate (Guarnieri et al. 2013). The measures at 4.5 mg/L are not reported herein because the particles were too diluted to give a good quality analysis. In addition, our DLS measurements indicated that there was no need to sonicate NPs suspensions before use. Sonication is expected to damage the particles to some extent producing fragments that could increase the polydispersity value of the NP sample, making the obtained results less accurate. The pH values of the PSNP solutions, in the absence of embryos, do not vary in time. In the presence of embryos, starting from the second day, the pH of the Ringer solution changes from 6.5 to 7, while the pH of the FETAX remains unchanged. The z-average of PSNPs, in FETAX solution, in the absence of embryos and at the concentrations of both 9 mg/L and at 18 mg/L reaches about 80 nm from the second day. In the presence of the embryos, the PSNPs showed strong aggregation up to about 300 nm (Tables 1, S2; Figs. 1, S1).

Concentration-dependent mortality

The embryos harvested in the presence of 18 mg/L PSNPs ($n = 225$) showed a percentage of mortality (about 20 %) similar to that found for control sibling embryos. In contrast, the embryos harvested in the presence of 9 mg/L PSNPs ($n = 225$) or 4.5 mg/L ($n = 225$) showed, respectively, 40 % and over 50 % of mortality rates (Table 2). These mortality values are statistically very relevant compared to those of the control sibling embryos ($n = 325$) (Table 2; Fig. 2a). Therefore, our data provide evidence that more pronounced PSNP dilutions produce mortality increase in these embryos (Fig. 2a). This correlation has been verified by Chi square test for trend ($P < 0.0001$; Table 2) and by the inverse linear relationship between the percentages of dead embryos and concentration ($P = 0.0345$, $r^2 = 0.9971$; Fig. 3a). To further analyze the effect of PSNPs on the embryos, we performed injections of PSNPs and/or GFP in one blastomere of *X. laevis* two-cell embryos for a total of 550 embryos. While the embryos injected with GFP alone ($n = 100$)

Table 1 Dynamic light scattering PSNPs in FETAX solution

Concentration	pH	Size (nm)	Size (SD)	Z-potential (mV)	Z-potential (SD)	PdI	PdI (SD)
9 mg/L; m0	7.4	55.62 ± 0.2285[a]	0.3958	−43.53 ± 0.2728[a]	0.4726	0.1593 ± 0.02009[a]	0.03479
9 mg/L; w/e; m1	7.5	82.83 ± 3.195[a]	5.534	−26.87 ± 1.707[a]	2.957	0.3800 ± 0.01914[a]	0.03315
9 mg/L; w/e; m2	7.5	88.61 ± 3.061[a]	5.302	−23.50 ± 2.003[a]	3.470	0.4647 ± 0.01530[a]	0.02650
9 mg/L; w/e; m4	7.5	78.40 ± 2.615[a]	4.530	−21.20 ± 2.458[a]	4.257	0.3570 ± 0.02931[a]	0.05076
9 mg/L; w/e; m7	7.5	101.1 ± 2.093[a]	3.625	−27.03 ± 2.585[a]	4.477	0.4670 ± 0.01744[a]	0.03020
9 mg/L; m1	7.5	116.6 ± 1.703[a]	2.950	−29.13 ± 2.859[a]	4.952	0.3693 ± 0.01337[a]	0.02316
9 mg/L; m2	7.5	224.5 ± 2.431[a]	4.210	−32.37 ± 3.624[a]	6.277	0.6217 ± 0.08284[a]	0.1435
9 mg/L; m4	7.5	466.0 ± 13.52[a]	23.41	−12.70 ± 0.4726[a]	0.8185	0.6787 ± 0.06701[a]	0.1161
9 mg/L; m7	7.5	1075 ± 26.65[a]	46.16	−10.87 ± 0.1856[a]	0.3215	1.000	
18 mg/L; m0	7.4	51.48 ± 0.2348[a]	0.4067	−34.9 ± 0.9644[a]	1.670	0.1097 ± 0.005667[a]	0.009815
18 mg/L; w/e; m1	7.5	62.52 ± 0.6393[a]	1.107	−25.57 ± 2.395[a]	4.148	0.2617 ± 0.01020[a]	0.01767
18 mg/L; w/e; m2	7.5	83.55 ± 0.7988[a]	1.383	−25.97 ± 2.589[a]	4.484	0.4323 ± 0.009615[a]	0.01665
18 mg/L; w/e; m4	7.5	71.51 ± 1.579[a]	2.736	−25.23 ± 0.3283[a]	0.5686	0.3383 ± 0.005783[a]	0.01002
18 mg/L; w/e; m7	7.5	84.99 ± 1.181[a]	2.045	−−26.00 ± 2.312[a]	4.004	0.3907 ± 0.03536[a]	0.06124
18 mg/L; m1	7.5	113.7 ± 21.86[a]	37.87	−30.73 ± 2.842[a]	4.922	0.5067 ± 0.1109[a]	0.1921
18 mg/L; m2	7.5	215.2 ± 2.193[a]	3.799	−30.97 ± 2.751[a]	4.765	0.4367 ± 0.007219[a]	0.01250
18 mg/L; m4	7.5	286.8 ± 13.43[a]	23.25	−21.63 ± 1.822[a]	3.156	0.4730 ± 0.06056[a]	0.1049
18 mg/L; m7	7.5	277.1 ± 3.782[a]	6.550	−10.91 ± 0.6996[a]	1.212	0.5617 ± 0.01135[a]	0.01966

[a] Mean value ± SE. $n = 3$

SD Standard Deviation *w/e* without embryos *mx* measure at day 'x' post fertilization

showed mortality similar to that of sibling embryos (Table 2), the injection of PSNPs produced mortality values of 66 % in embryos injected with 4.5 mg/L, 70 % in embryos injected with 9 mg/L, and of 80 % in embryos injected with 18 mg/L (Table 2; Fig. 2b). According to the Chi square test for trend, the observed mortality increase is dose dependent ($P = 0.0035$; Table 2). The graph in Fig. 3b shows direct correlation between mortality and concentration of nanoparticles injected ($P = 0.0334$, $r^2 = 0.9973$).

PSNPs affect embryo phenotype

PSNPs microinjected or contacted embryos produced the same type of abnormalities in developing embryos (Figs. 4, 5). These malformations concern derivatives of all three germ layers: ectoderm, endoderm, and mesoderm. Deformations of the tail were observed with regard to length, shape, and number (4–50 %) (Figs. 4 a–c, 5b, d, e, h; Table 3) (Gont et al. 1993). Embryos showed various abnormalities of the head (13–37 %) (Fig. 5a; Table 3) as small eyes (Fig. 4g), the absence of or variously deformed eyes (Fig. 5b, c, e, f, h), and cone-shaped eyes (Fig. 5b, e, f).

Sections carried out through the head showed abnormalities to the retina layers and malformations of the corresponding encephalon in contact-embryos (Fig. 5f–g). Abnormalities were observed also in epidermal melanocytes, which were randomly distributed and often clustered (13–28 %) (Figs. 4d, 5e; Table 3) and in the winding of the intestine that appeared immature with respect to control sibling tadpoles (13–36 %) (Figs. 4 e–g, 5c, d, h; Table 3) (Chalmers and Slack 1998). Moreover, the contacted and microinjected embryos showed variously extended edema in the ventral anterior zone (6–24 %) (Figs. 4g, 5b, c, d, h; Table 3). Head malformations and edema were not observed in 4.5 mg/L contact embryos at stages 41–45 when the counts were performed (Table 3). The total absence in these embryos of head malformation or edema correlates with the high percentage of mortality presented early in development which starts from the neurula stage. At that stage, these embryos showed malformations of the prospective head so severe and an edema so extensive, which were incompatible with embryo survival (data not shown). Instead, by comparing mortality results in Tables 2, 3, it is evident that

the survived embryos are the ones that showed comparable malformations. In both treatments, embryos often displayed more than one of the mentioned malformations: we define 'severe' malformed embryo when the phenotypes display two malformations, and 'monster' when the phenotypes carry at least three malformations, thus rendering it difficult to recognize their original pattern of development. In particular, contact embryos treated with 18 mg/L grew more slowly than sibling embryos and show 27 % monster phenotypes (Table 3). Moreover, the 9 mg/L and the 18 mg/L contacted embryos were

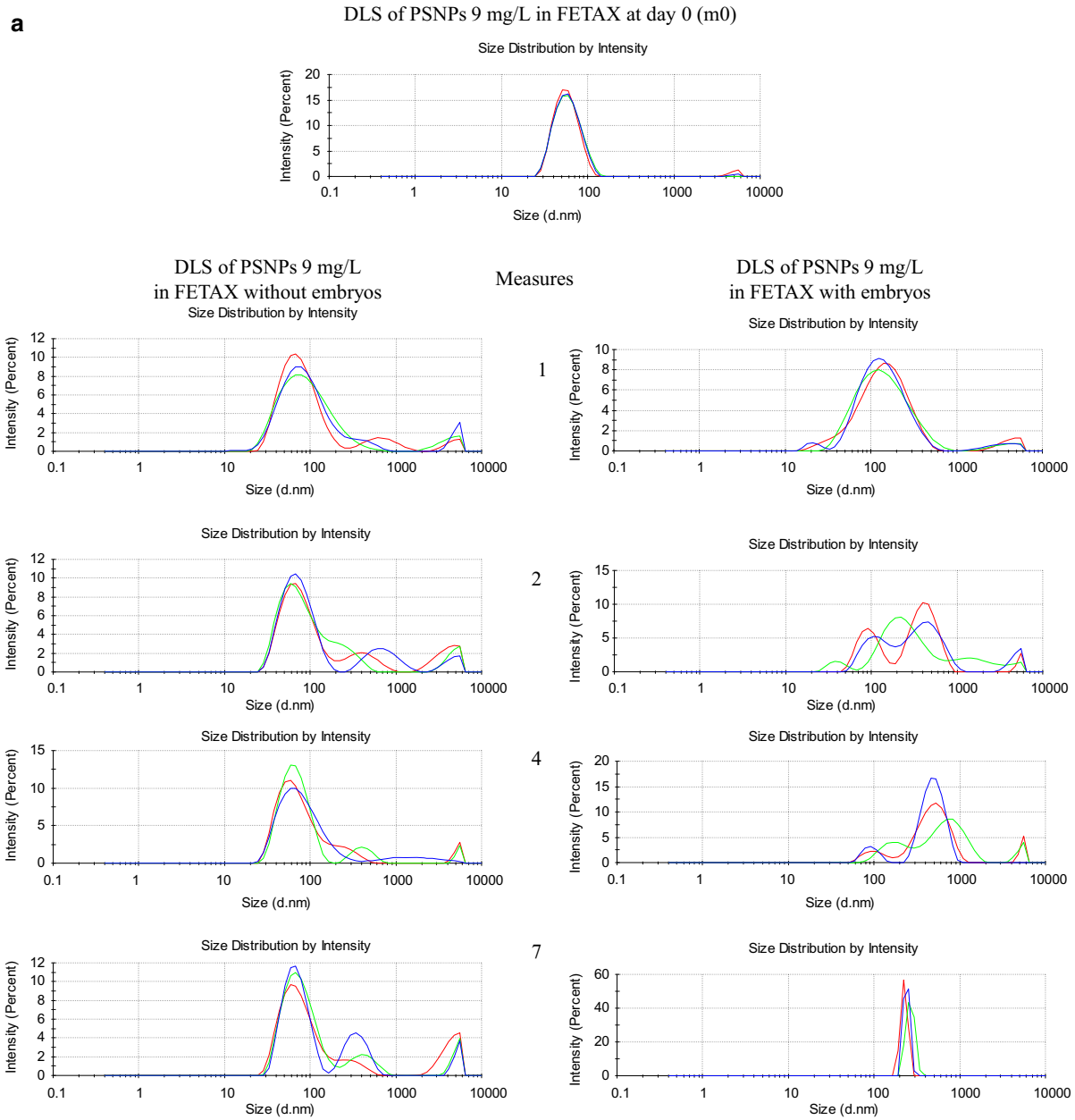

Fig. 1 Graphs of the PSNP solutions measurements performed at the DLS. Each curve represents the average of five measurements, each performed in triplicate without embryos (**a**, **b**, *left*) or with embryos (**a**, **b**, *right*). In both cases, it is possible to observe a time dependent appearance of the peaks related to the increasing size of the particles. In the solution with embryos the PSNPs increase begins earlier and is more evident than in the solution without embryos

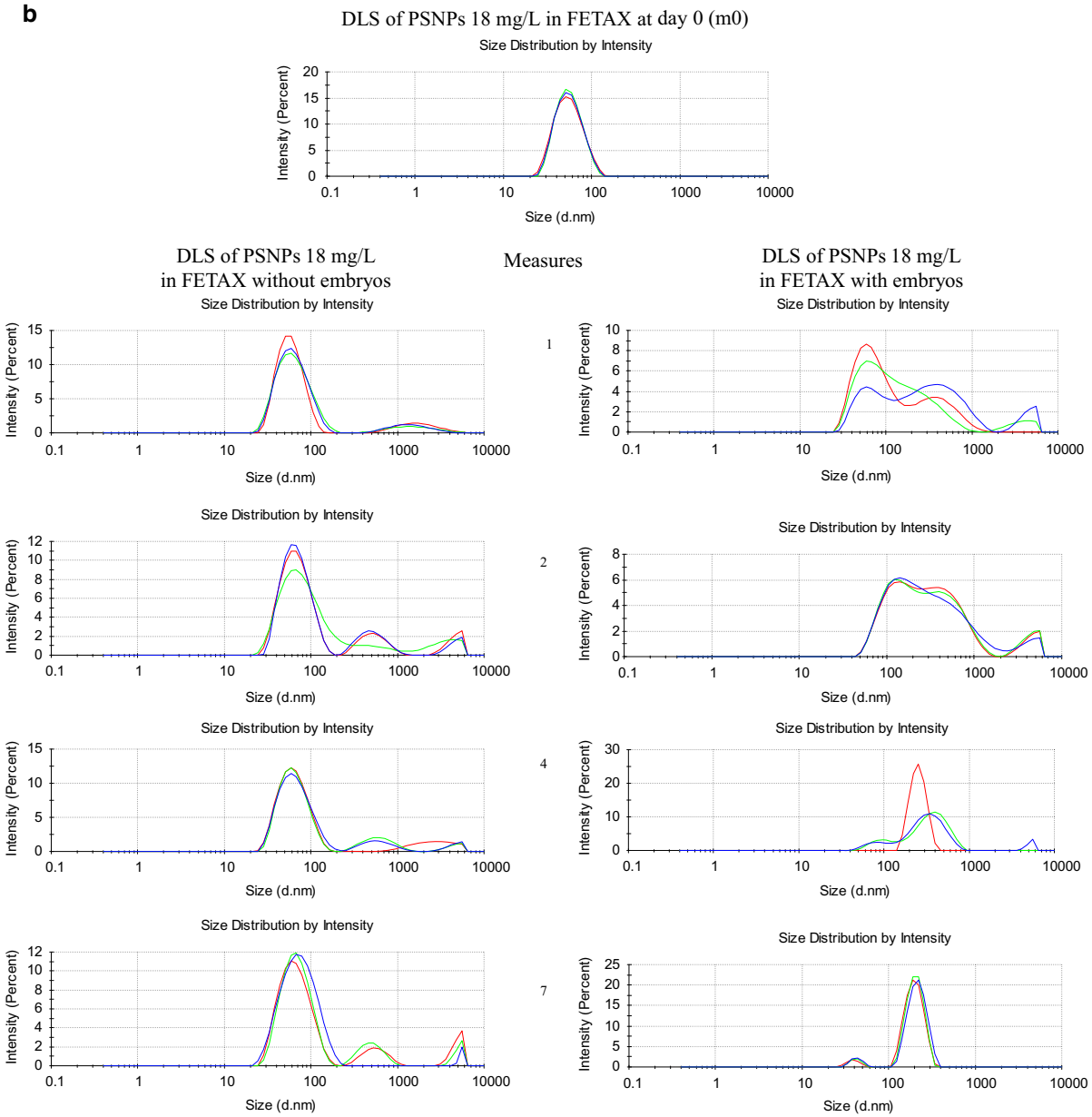

Fig. 1 continued

significantly shorter than the control embryos (Fig. 6). Embryos microinjected in one blastomere of two-cell stage showed the amended phenotype in both the injected and the noninjected side (Table 3). In *Xenopus*, the first two cells give rise to the left and right sides of the embryo. While microinjection of GFP had no effect on the embryos development as shown in Fig. 4h, the PSNPs microinjected embryos showed modification on both the left and right sides, thus indicating that the injected PSNPs pass from one cell to another affecting the development of the whole embryo. The red fluorophore conjugated to nanoparticles allowed us to use the confocal microscopy to observe their localization in the various embryonic districts. PSNPs exposed embryos fixed at stage 45–46 show aggregates of PSNPs in the digestive tract (Fig. 7a–a_3), in the eyes (Fig. 7b–b_3) and in the pharynx (Fig. 7c–c_4), but not in the brain (Fig. 7c–c_2).

Table 2 Embryotoxic effects in *X. laevis*

	Contact embryos				Injected embryos			
	Control	4.5 (mg/L)	9 (mg/L)	18 (mg/L)	GFP	4.5 (mg/L)	9 (mg/L)	18 (mg/L)
Utilized embryos (n)	325	225	225	225	100	100	100	250
Dead embryos (n)	57	119	89	41	25	66	70	200
Living larvae (n)	268	106	136	184	75	34	30	50
Mortality (%)	17.54	52.8[a,b]	39.6[a,b]	18.2[b]	25	66[a,c]	70[a,c]	80[a,c]
Malformation n	4	49	95	137	1	23	21	42
Malformation (%)	1.49	46.2[a,b]	69.8[a,b]	74.46[a,b]	1.33	67.6[a,b]	70[a,b]	84[a,b]

n number

[a] Chi square test; $P < 0.0001$

[b] Chi square test for trend; $P < 0.0001$

[c] Chi square test for trend; $P = 0.0035$

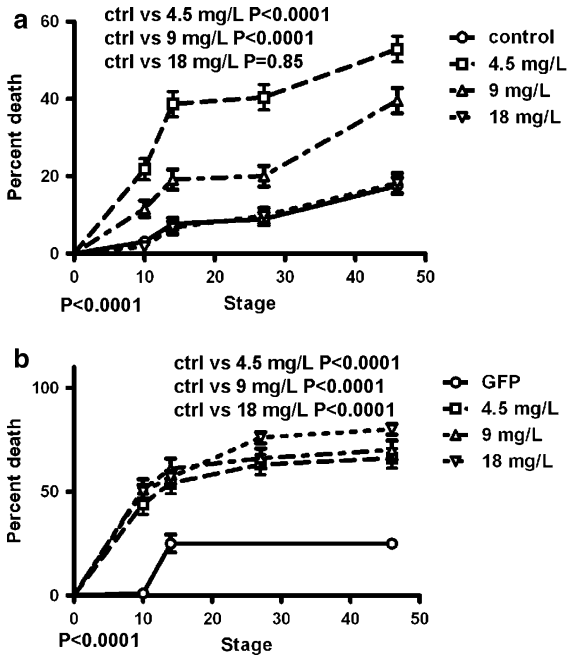

Fig. 2 Mortality evaluation in PSNP-treated embryos. The mortality distributions were evaluated by non-parametric Mantel-Cox test (**a** contact embryos) giving $P > 0.05$ (PSNPs treatment with 18 mg/L compared with the control; $P = 0.85$) and $P < 0.0001$ (PSNPs treatment with 9 or 4.5 mg/L compared with control). **b** Injected embryos: PSNPs treatment with 18 or 9 or 4.5 mg/L in respect to control show $P < 0.0001$. The experimental points represent the average from nine independent experiments for contact embryos and five experiments for injected embryos. The *error bars* indicate the standard error

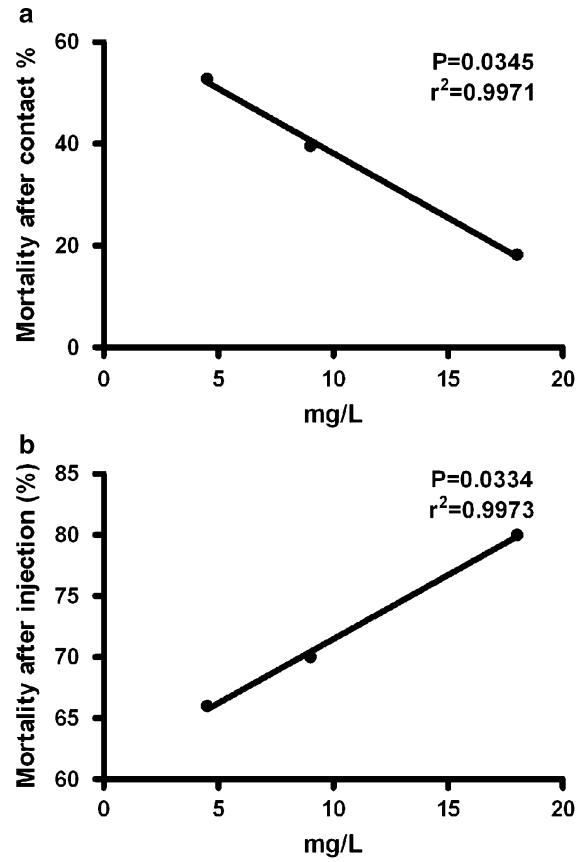

Fig. 3 Correlation between mortality and PSNPs concentrations upon contact and injection. **a** Correlation between mortality percentage and PSNPs concentrations in contact embryos ($P = 0.0345$, $r^2 = 0.9971$) and **b** injected embryos ($P = 0.0334$, $r^2 = 0.9973$)

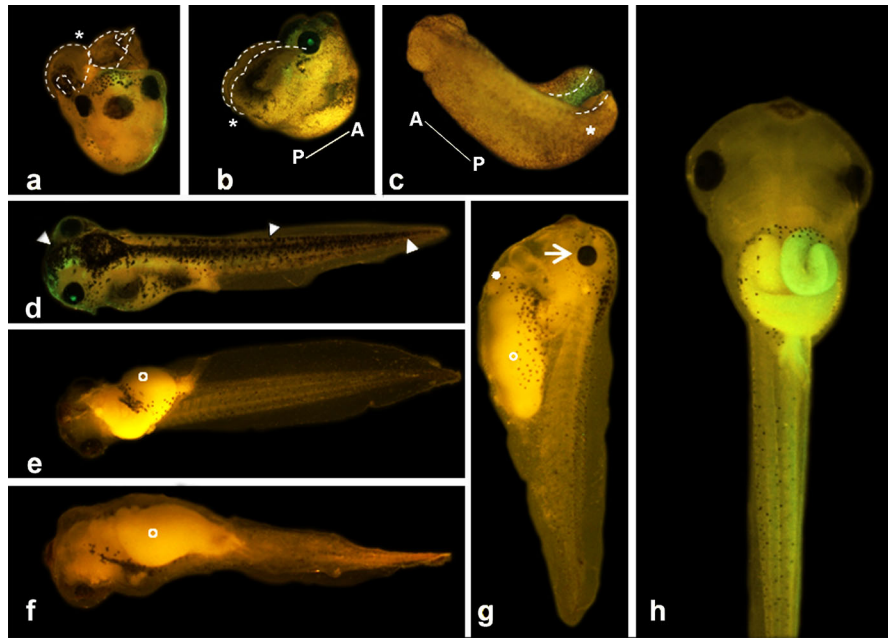

Fig. 4 PSNPs injection effects on embryos development. **a–g** Embryos injected with PSNPs and GFP mRNA into one blastomere at two-cell stage and harvested until stage 45/46. The injected side is marked by GFP. **a–c** The embryos show a reduced length and a forked tail (*dashed lines*). In **c** the embryo is caught at about stage 25 when it stopped growing. **d** Embryo showing abnormal distribution of pigment (*dorsal view, arrowheads*). **e–f** Embryos (*ventral view*) showing an immature gut (*circle*) compared with sibling embryos at the same stage of growth (see **h**). **g** Embryo with small eye (*arrow*), edema (*spot*) and primitive gut (*circle*). **h** Control sibling embryo injected only with GFP mRNA

In the intestine, the aggregates were present both in its lumen and in its wall (Fig. 7a–a_2), as shown in particular in Fig. 7a_3. Pharynx presents PSNPs aggregates of various sizes (Fig. 7c–c_4). In the eyes, PSNPs are found around the lens and between the pigmented layer and the outer layer of retina (ONL) (Fig. 7b–b_3), as well as in the optic nerve evenly distributed throughout the structure (Fig. 7b–b_3). The images in Fig. 7 show that the NPs assayed can penetrate in all embryonic tissues if in direct contact. Magnification of digestive tract cells showed the presence of the PSNPs in the cytoplasm, in the nucleus, and in the cellular periphery (Fig. 7d). The aggregates are more abundant in the gut tissue with respect to the pharynx and the eyes (Fig. 7e).

Expressions of *bra*, *myod1*, and *sox9* mRNAs are amended in embryos treated with PSNPs

The malformations observed in embryos treated with PSNPs led us to investigate whether also an altered expression of genes is involved in the early embryonic development. Nanoparticles can induce changes in gene expression (Fan et al. 2012). For this purpose, we used *bra* (early mesoderm marker), *myod1* (paraxial mesoderm marker), and *sox9* (neural crests migration marker). We performed the hybridizations of *bra* and *myod1* mRNAs, on PSNPs injected (Fig. S2 a'–c' for riboprobes *bra* and d'–f' for *myod1*) and control, uninjected sibling embryos (Fig. S2 a–c for *bra* and d–f for *myod1*). The latter expressed *bra* in the marginal zone shortly before the beginning of gastrulation in a crown-shaped pattern (Fig. S2 a). During gastrulation, transcription of *bra* was maintained in the prospective notochord along the A/P axis (Fig. S2 b) and, at the end of gastrulation, *bra* could be detected mostly in the notochord and in the posterior mesoderm (Fig. S2 c) (Smith et al. 1991; Kwan and Kirschner 2003). In PSNPs injected embryos (Fig. S2 a'–c') at the beginning of gastrulation, a partial expression of *bra* was observed that did not cover the entire marginal zone (Fig. S 2a') suggesting changes in the migration of the prospective mesoderm that did not fully migrate to form a complete notochord (Fig. S2 b'). At the neurula stage, the notochord appeared displaced sideways (Fig. S2 c'). In similarly microinjected embryos, the

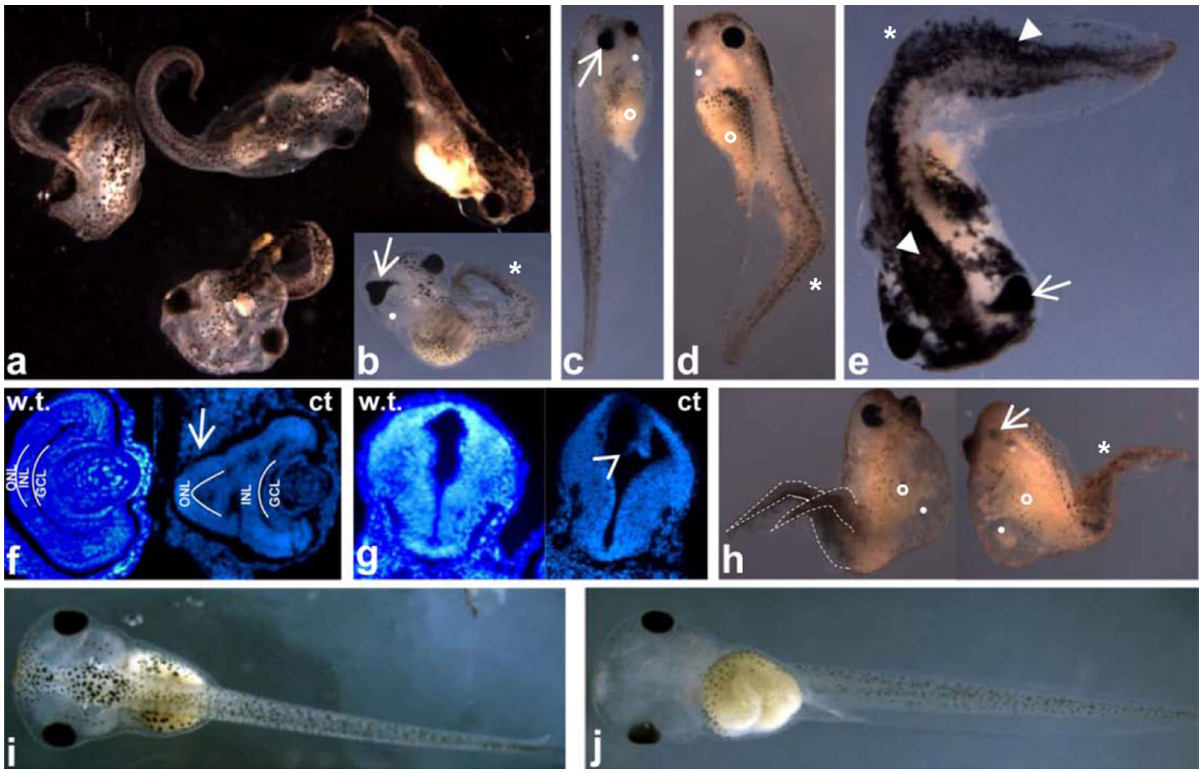

Fig. 5 PSNPs contact effects on embryos development. **a** Set of stage 45/46 embryos showing anomalies of different types. **b–d, h** Embryos with edema in ventral anterior zone (*spot*), **b, c, e, h** embryos with different anomalies of eyes (*arrow*), **b, d, e, h** embryos with anomalies of the tail (*asterisk*), **c, d**, **h** embryos with abnormal intestine (circle), **e** embryos with anomalous pigment distribution (*arrowheads*). DAPI staining of cryostat sections of exposed embryos, showing irregular stratification of retina in **f** (*arrow*, *white lines define retina layers*: *ONL* outer nuclear layer, *INL* inner layer, and *GCL* ganglion cell layer) and in **g** malformation of neural tube (*empty arrowhead*), compared with wild types. **h** Right and left views of a st. 41 embryo are shown. The embryo misses one eye (*arrow*) and displays anomalies of the tail (*dashed lines*) and of the intestine (*circle*) as well as an edema (*spot*). **i–j** Wild-type st.45 embryo in dorsal **i** and ventral views **j**

myod1 expression was displaced as well (Fig. S2 d'–f'). During gastrulation, *myod1* localization did not have the typical horseshoe shape (compare Fig. S2 d with Fig. S2d'). The expression of *myod1* was altered also later at the early stage of neurula, where the expression was rather asymmetric in contrast to wild-type embryos (Fig. S2 e–e') and at stage 25, where the riboprobe localization extended up to the head (Fig. S2 f–f') (Hopwood et al. 1989, 1992; Scales et al. 1990).

Abnormalities in the migration of the neural crest, which is currently regarded as a germ layer, were assessed employing *sox9* riboprobe. Untreated embryos (Fig. S3 a–b) expressed this messenger at the levels of the branchial arches (Fig. S3 a–b,), facial cartilage (Fig. S3 b), olfactory bulbs (Fig. S3 b), and epidermis (Fig. S3 a–b) (El Jamil et al. 2008; Spokony et al. 2002). Stage 46 contact-embryos exhibited altered expression of *sox9* mRNA. In these embryos, *sox9* showed anomalous and variable expressions in the epidermis and in the malformed gut (Fig. S3 d–e). In the eyes, a strong hybridization is detected in the retina (Figs. S3 e). Little *sox9* expression was found in the underdeveloped branchial arches region (Fig. S3 c–d) and in the misplaced olfactory bulbs (Fig. S3 c).

Discussion

The impact of nanostructured products on the ecosystem is not completely clear, albeit some preliminary reports led to reasons of full concern (Kumar et al. 2012; Scown et al. 2010). In particular, the potential

Table 3 Pattern malformations in *X. laevis*

	Contact embryos				Injected embryos			
	Control	4.5 (mg/L)	9 (mg/L)	18 (mg/L)	GFP	4.5 (mg/L)	9 (mg/L)	18 (mg/L)
Gut n (%)	1 (0.37)	27 (25.47)[d]	30 (22.05)[d]	46 (25)[d]	0	8 (23.529)[d]	4 (13.33)[b]	18 (36)[d]
Pigment n (%)	3 (1.12)	18 (16.98)[d]	18 (13.23)[d]	50 (27.17)[d]	0	0	4 (13.33)[b]	14 (28)[d]
Tail n (%)	0	4 (3.77)[b]	23 (16.91)[d]	59 (32.06)[d]	1 (1.33)	18 (52.94)[b]	6 (20)[c]	9 (18)[c]
Head n (%)	0	0	38 (27.94)[d]	68 (36.95)[d]	0	0	4 (13.3)[b]	7 (14)[c]
Edema n (%)	0	0	9 (6.61)[d]	14 (7.61)[d]	0	5 (14.7)[c]	3 (10)[a]	12 (24)[d]
Monster n (%)	0	0	9 (6.6)	50 (27.17)	0	1 (2.94)	2 (6.6)	9 (18)
Severe n (%)	0	0	5 (3.67)	0	0	6 (17.64)	1 (3.3)	0

Percentages based on number of malformations/number of the living *n* number

[a] Chi square test; $P < 0.05$

[b] Chi square test; $P < 0.01$

[c] Chi square test; $P < 0.001$

[d] Chi square test; $P < 0.0001$

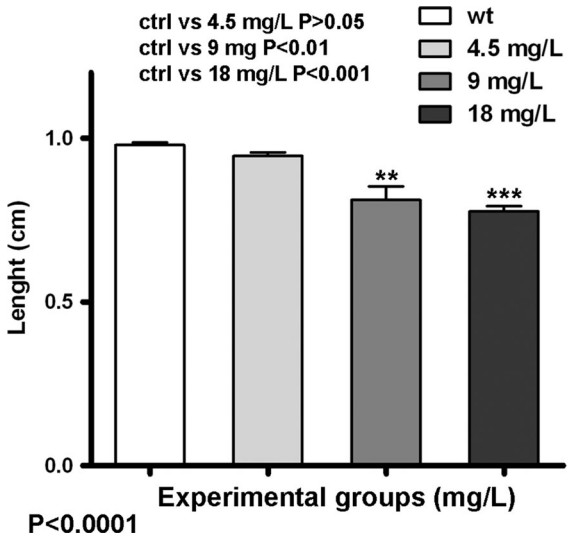

Fig. 6 Growth retardation analysis. The growth retardations were evaluated with ANOVA statistical test giving $P < 0.0001$. 18 mg/L versus control: $P < 0.001$; 9 mg/L versus control: $0.001 < P < 0.01$ and 4.5 mg/L versus control: $P > 0.05$. The *error bars* indicate the standard error

embryotoxic effects of NPs on both aquatic organisms (Bacchetta et al. 2012; Casado et al. 2013; Krysanov et al. 2010) and laboratory mammals (Bosman et al. 2005; Tian et al. 2009) deserve full attention. NPs may in fact constitute a serious danger not only for these organisms, but also for their consequent domino effects, in particular along the aquatic food chain (Cedervall et al. 2012). To improve the understanding of this topic, in the present study, we investigate the potential effects of the PSNPs accumulation in *X. laevis* embryos for the assessment of their effects on aquatic larvae in view of their possible employments in future studies (Chang 2010). In particular, we have tested uncoated fluorescent of about 50 nm PSNPs because it is well known that maximal cellular uptake of NPs can take place in the intermediate size range of 40–60 nm and that fluorescence offers an efficient tracking method (Nam et al. 2013). We have employed a range of concentrations that have been used to test these NPs in other organisms (Casado et al. 2013) applying the FETAX protocol (Bacchetta et al. 2012; Bantle and Dawson 1988).

DLS data show that at the beginning of the experiment, the PSNPs utilized have a diameter of about 54 nm in amphibian Ringer or FETAX. Analyses of the mortality in contacted-embryos suggest that they die depending on the nanoparticles concentration; the mortality is inversely dependent on NPs concentration. Apparently, these data are in contrast with the literature (Casado et al. 2013). Mortality increases observed in contact-embryos suggest that the NPs penetrate more efficiently at a lower concentration. Higher concentrations of PSNPs produce aggregates before entering the embryos more readily than at lower concentrations. Our data show that the PSNPs at the concentrations of both 9 and 18 mg/L, starting from the second day, aggregate in the presence of the embryos. The PSNPs at the concentration of 4.5 mg/L

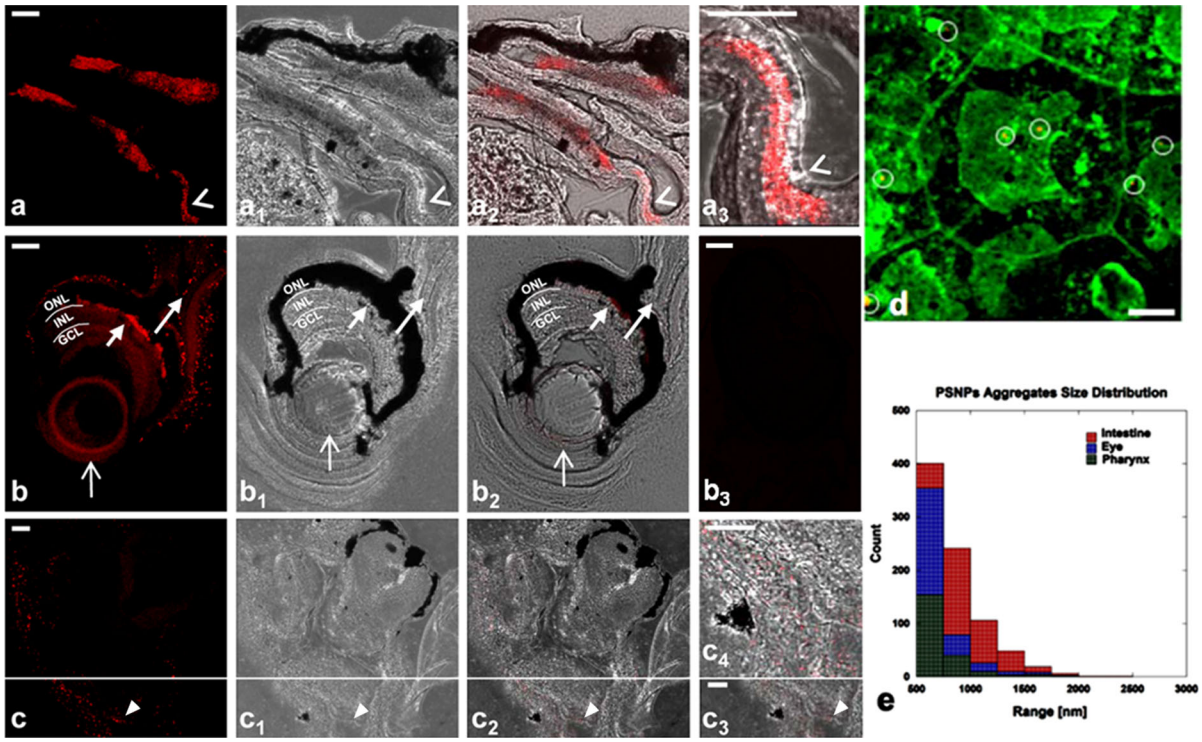

Fig. 7 PSNPs confocal localization. The distributions of PSNPs in the intestine **a**–**a**$_3$, in the eye **b**–**b**$_3$, and in the brain/pharynx **c**–**c**$_4$ are here shown by confocal microscopy. Figures **a**–**c** shows fluorescent optical sections; figures **a**$_1$–**c**$_1$ shows the same sections in brightfield and figures; **a**$_2$–**c**$_2$ shows the merge between them. In **a**$_3$ is shown an enlargement of the area indicated by the *empty arrowhead* in **a**–**a**$_2$; the nanoparticles are in the tissue (**a**$_3$, *empty arrowhead*). In the eyes **b**–**b**$_2$; nanoparticles are distributed in the ONL of the retina (*short arrow*), in lens (*thin arrow*), and in the optic nerve (*arrow*); *white lines* define retina ONL, INL, and GCL. In **b**$_3$ is shown the control optical section. In **c**–**c**$_2$, the brain does not show aggregates of PSNPs (see the area over the *white line*), while in the pharyngeal area **c**–**c**$_4$ (see the area under the line that was used to highlight the zone), there are interspersed aggregates of nanoparticles (*arrowhead*). A contrast-enhanced image of merge **c**$_3$ together with a magnification **c**$_4$ of pharynx area (*arrowhead*) confirms the presence of fluorescent aggregates. In **d** magnification of the gut cells, stained with WGA-FITC conjugated, shows the PSNPs. The *red-yellow* PSNPs are seen in the cytoplasm, in the nucleus, and at the cell periphery (*circle*). In **e** the histogram shows the aggregates size distribution in intestine (*red*), eye (*blue*), and pharynx (*green*). **a**–**a**$_3$, **b**–**b**$_3$, and **c**–**c**$_4$ *scale bar* = 50 μm, **d** *scale bar* = 5 μm. (Color figure online)

cannot be measured using the DLS. The fact that we have observed large aggregates of PSNPs by confocal microscopy at the tissue borders argues in favor of this hypothesis. It should also be mentioned that, in contact-embryos, the aggregates penetration may be slowed down by envelopes covering the embryos. In fact, when PSNPs were added at two-cell stage, they have to pass through the vitelline envelope, an extracellular barrier that accompanies the embryos until stage 32, and in later stages, they have to pass the tegument. In the injected embryos, the mortality rate increases according to the increment of PSNPs amount. This increase is statistically significant. Based on our data, microinjections appear a particularly appealing method for investigating PSNPs effects, as the amount of the administered PSNPs is more likely to reach the embryo cytoplasm in unmodified conditions, and we are sure that nanoparticles are inside the embryos. Comparing the effects obtained with both techniques, we could understand that the effects we observed in contact embryos are due to PSNPs, as they are the same in both kind of treatments. Interestingly, although embryos were microinjected only in one side, the effects on the phenotype are present in both the injected and the noninjected sides, indicating that the PSNPs can pass from one cell to another. Lai et al. (2007) showed that 24-nm polymer nanoparticles can exploit a non-clathrin, non-caveolae, and cholesterol-independent pathway for nondegradative trafficking. Moreover, polystyrene microspheres ranging from

50 nm to 3 μm fed to female rats are absorbed into the gastrointestinal tract, but particles larger than 100 nm do not reach the bone marrow, and those larger than 300 nm are absent from blood and do not penetrate the tissues (Jani et al. 1990). However, it should be mentioned that the observations made on contact embryos where the PSNPs might have been modified through transporting process from extracellular to intracellular environment may represent more valid information for environmental studies than observations made through directly injected PSNPs (Xu et al. 2014). We showed that PSNPs treated groups, contacted or injected, display the same modifications statistically relevant and higher compared with controls in pigment distribution, malformations of the head, tail, and edema in the anterior ventral region and of the gut winding. Moreover, these malformations can be variously associated. They create embryos with phenotypes dramatically different from the wild type (monsters) or induce their mortality. In addition, the embryos grew more slowly than the sibling embryos. PSNPs aggregates were observed particularly in the intestine, in accordance with the fact that at stage 40/41 *X. laevis* embryos opened their mouth and ingestion becomes the main route of PSNPs intake. In particular, we have showed that PSNPs entered the gut mucosa, the eyes, and the pharynx and were distributed in the cytoplasm and in the nucleus indicating that they can penetrate easily into the cells. Moreover, the diencephalon anomalies we observed might have been caused by small amount of particles, in a quantity not detectable by our methods, or indirectly by the surrounding tissues. Interestingly, Symens et al. (2011), using the *Xenopus* nuclear envelope reassembly assay, found that the nuclear enclosure of nanoparticles they observed were dependent on size and charge of the polystyrene beads. The delayed distribution or non placement of specific mRNAs we showed in PSNPs injected embryos during early development may cause the abnormal development observed in treated embryos, including the tail formation that develops as a direct continuation of events initiated during gastrulation (Gont et al. 1993). *Brachyury* expression characterizes the migratory mesodermic cells of vertebrates and is required for mesoderm formation in *Xenopus*, an indispensable component of all the organs (Yanagisawa et al. 1981; Smith et al. 1991). *myod* expression is involved in the activation of muscle genes in the somites of embryos (Taylor et al. 1991), *sox9* incorrect localization could produce a defect in the migratory activity of the neural crest multipotent cells first located at the lateral edges of the neural plate. As they reach their targets, neural crests differentiate in various cell types, including epidermal melanocytes (Le Douarin and Creuzet 2011) and several malformations we observed in the treated embryos, such as defects in pigmentation are in agreement with neural crests incorrect migration. These data suggest that, at the experimental concentrations we used, the 50 nm PSNPs have a toxic and a possible additional teratogenic potential, in contrast to the fact that the polystyrene is an inert material. Thus, PSNPs cannot be considered as a simple neutral vehicle when in living cells. This conclusion should be taken in account before using PSNPs for medical treatments, as suggested by recent literature on airway cells (McCarthy et al. 2011), intestinal epithelium (Mahler et al. 2012) and blood coagulation (Oslakovic et al. 2012) all depending in different ways on PSNPs size and surface chemistry (Cedervall et al. 2007; Lundqvist et al. 2008). In particular, modified PSNPs induce a growth inhibition of the mouse embryos (Tian et al. 2009) similar to the effect we remarked in *Xenopus*. Several NPs (i.e., silver, gold and silica NPs) are able to overpass the embryonic barriers and to penetrate zebrafish embryos even at early stages, thus contributing to generate adverse developmental effects (Lee et al. 2007; Browning et al. 2009; Fent et al. 2010).

In a biological fluid, nanoparticles are not naked but covered with a protein "corona" which mediates the biological effects of NPs and changes over time as it moves from one fluid compartment to another (Dell'Orco et al. 2010; Xu et al. 2014). A remarkable specificity in the composition of the "corona" depending on NPs size and surface chemistry was shown (Lundqvist et al. 2008, 2011). Proteins in the "corona" may perturb aggregate structures (Cabaleiro-Lago et al. 2010), produce loss or gain of function (Oslakovic et al. 2012) or an increased inflammatory response (Chang 2010). These effects are comparable to those that PSNPs produce in our experiments, suggesting that the "corona" effect may occur in *Xenopus* blastomeres, as shown in other studies (Cedervall et al. 2012; Xu et al. 2014).

In addition, the effects we observed may depend on the "mechanical stress" induced by the large quantity of PSNPs that accumulate in the embryonic anlagen (Bacchetta et al. 2012). Significant malformations in

the intestine of *X. laevis* treated with TiO_2 NPs, that do not release toxic metal ions similarly to PSNPs (Yamamoto et al. 2004), may be caused by "mechanical stress" due to the large quantities of TiO_2 released in the digestive tract (Bacchetta et al. 2012). PSNPs microinjections at the beginning of the development appear to displace mRNAs which is important in the early stages of the development. The effects produced may depend on the change of gene expression induced by PSNPs (Fan et al. 2012) or "mechanical stress" resulting from the large quantity of PSNPs or to threshold concentrations able to affect tissues. If the latter hypothesis were correct, this would imply that PSNPs might interfere with mechanisms of cellular movements, thus contributing to cause the observed potential teratogenic effect. Further studies are necessary to minimize the effects of these NPs.

Conclusions

In conclusion, our data suggest that PSNPs aggregation in solution can depend not only on pH but also on the presence of embryos. In embryos, in spite of the different methods of PSNPs administration, we detected, in both cases, anomalous distribution of pigmentation; malformations of the head, gut, and tail; edema in the anterior ventral zone; and a shorter body length compared with the wild type; these anomalies were variously distributed in treated embryos. Moreover, the treated embryos showed an increase in mortality and grew more slowly than control sibling embryos. Confocal microscopy of contact-embryos showed PSNPs in the intestinal cells, while in other organs, PSNPs were not observed. We found an anomalous distribution of the genes involved in the early embryonic development and neural crest migration. The results of our research show that the PSNPs we used produce malformations despite the presumed inert chemical properties of the polystyrene bulk and indicate that the lethal effect of PSNPs depends both on exposure concentration level and on the ability they have to penetrate the tissue. Our data also demonstrate that the tests we used in *Xenopus* may be powerful and flexible bioassays for evaluation of pollutants in aquatic embryos.

Acknowledgments The authors wish to thank C. Campanella for her suggestions, and A. Fazzolini for laboratory assistance. This work was supported by the Grant FARO (Finanziamento per l'Avvio di pROgetti Speciali) and by the departmental research funding (Project: A10113.CRRDI; F.S.2.18.03).

References

Bacchetta R, Santo N, Fascio U, Moschini E, Freddi S, Chirico G, Camatini M, Mantecca P (2012) Nano-sized CuO, TiO_2 and ZnO affect *Xenopus laevis* development. Nanotoxicology 6(4):381–398

Bantle JA, Dawson DA (1988) Uninduced rat liver microsomes as a metabolic activation system for the frog embryo. In: Adams WJ, Chapman GA, Landis WF (eds) Aquatic toxicology and hazard assessment, ASTM STP 971. ASTM, Philadelphia, p 316

Bosman SJ, Nieto SP, Patton WC, Jacobson JD, Corselli JU, Chan PJ (2005) Development of mammalian embryos exposed to mixed-size nanoparticles. Clin Exp Obstet Gynecol 32(4):222–224

Browning LM, Lee KJ, Huang T, Nallathamby PD, Lowman JE, Xu XN (2009) Random walk of single gold nanoparticles in zebrafish embryos leading to stochastic toxic effects on embryonic developments. Nanoscale 1:138–152

Cabaleiro-Lago C, Lynch I, Dawson KA, Linse S (2010) Inhibition of IAPP and IAPP(20–29) fibrillation by polymeric nanoparticles. Langmuir 26:3453–3461

Casado MP, Macken A, Byrne HJ (2013) Ecotoxicological assessment of silica and polystyrene nanoparticles assessed by a multitrophic test battery. Environ Int 51(2013):97–105

Cedervall T, Lynch I, Foy M, Berggård T, James P et al (2007) Detailed identification of plasma proteins absorbed to copolymer nanoparticles. Angew Chem Int Ed 46:5754–5756

Cedervall T, Hansson L-A, Lard M, Frohm B, Linse S (2012) Food chain transport of nanoparticles affects behaviour and fat metabolism in fish. PLoS One 7(2):e32254. doi:10.1371/journal.pone.0032254

Chalmers AD, Slack JMW (1998) Development of the gut in *Xenopus laevis*. Dev Dynam 212:509–521

Chang C (2010) The immune effects of naturally occurring and synthetic nanoparticles. J Autoimmun 34:234–246

Dell'Orco D, Lundqvist M, Oslakovic C, Cedervall T, Linse S (2010) Modelling the time evolution of the nanoparticle-protein corona in a body fluid. PLoS One 5:e10949

Dumont JN, Schultz TW, Buchanan M, Kao G (1983) Frog embryo teratogenesis assay-*Xenopus* (FETAX)–a short–term assay applicable to complex environmental mixtures. In: Waters MD, Sandhu SS, Lewtas J, Claxton L, Chernoff N, Nesnow S (eds) Short-term bioassays in the analysis of complex environmental mixtures. Plenum Press, New York, pp 393–405

El Jamil A, Kanhoush R, Magre S, Boizet-Bonhoure B, Penrad-Mobayed M (2008) Sex-specific expression of *sox9* during gonadogenesis in the amphibian *Xenopus tropicalis*. Dev Dyn 237(10):2996–3005

Enright HA, Bratt JM, Bluhm AP, Kenyon NJ, Louie AY (2013) Tracking retention and transport of ultrafine polystyrene in an asthmatic mouse model using positron emission tomography. Exp Lung Res 39(7):304–313

Fan Z, Yang X, Li Y, Li S, Niu S, Wu X, Wei J, Nie G (2012) Deciphering an underlying mechanism of differential cellular effects of nanoparticles: an example of Bach-1 dependent induction of HO-1 expression by gold nanorod. Biointerphases 7(1–4):10. doi:10.1007/s13758-011-0010-x

Fent K, Weisbrod CJ, Wirth-Heller A, Pieles U (2010) Assessment of uptake and toxicity of fluorescent silica nanoparticles in zebrafish (Danio rerio) early life stages. Aquat Toxicol 100:218–228

Fleischer CC, Payne CK (2014) Secondary structure of corona proteins determines the cell surface receptors used by nanoparticles. J Phys Chem B 118(49):14017–14026

Gont LK, Steinbeisser H, Blumberg B, De Robertis EM (1993) Tail formation as a continuation of gastrulation: the multiple cell populations of the *Xenopus* tailbud derive from the late blastopore lip. Development 119(4):991–1004

Guarnieri D, Guaccio A, Fusco S, Netti PA (2011) Effect of serum proteins on polystyrene nanoparticle uptake and intracellular trafficking in endothelial cells. J Nanopart Res 13:4295–4309. doi:10.1007/s11051-011-0375-2

Guarnieri D, Falanga A, Muscetti O, Tarallo R, Fusco S, Galdiero M, Galdiero S, Netti PA (2013) Shuttle-mediated nanoparticle delivery to the blood-brain barrier. Small 9(6):853–862

Hardy CL, Lemasurier JS, Mohamud R, Yao J, Xiang SD, Rolland JM, O'Hehir RE, Plebanski M (2013) Differential uptake of nanoparticles and microparticles by pulmonary APC subsets induces discrete immunological imprints. J Immunol 91(10):5278–5290

Hopwood ND, Pluck A, Gurdon JB (1989) MyoD expression in the forming somites is an early response to mesoderm induction in *Xenopus* embryos. EMBO J 8(11):3409–3417

Hopwood ND, Pluck A, Gurdon JB, Dilworth SM (1992) Expression of XMyoD protein in early *Xenopus laevis* embryos. Development 114(1):31–38

Jani P, Halbert G, Langridge J, Florence A (1990) Nanoparticle uptake by the rat gastrointestinal mucosa: quantization and particle size dependency. J Pharm Pharmacol 42:821–826

Kahru A, Dubourguier H-C (2010) From ecotoxicology to nanoecotoxicology. Toxicology 269:105–119

Krysanov EYu, Pavlov DS, Demidova TB, Dgebuadze YuYu (2010) Effect of nanoparticles on aquatic organisms. Biol Bull 37:406–412

Kumar C (2006) Nanomaterials: toxicity, health, and environmental issues. In: Kumar C (ed) Nanotechnologies for the Life Sciences Vol 5, 1st edn. Weinheim, Wiley-VCH, pp 393–405

Kumar V, Kumari A, Guleria P, Yadav SK (2012) Evaluating the toxicity of selected types of nanochemicals. Rev Environ Contam Toxicol 215:39–121. doi:10.1007/978-1-4614-1463-6_2

Kwan KM, Kirschner MW (2003) X*bra* functions as a switch between cell migration and convergent extension in the *Xenopus* gastrula. Development 130:1961–1972

Lai SK, Hida K, Man ST, Chen C, Machamer C, Schroer TA, Hanes J (2007) Privileged delivery of polymer nanoparticles to the perinuclear region of live cells via a non-clathrin, non-degradative pathway. Biomaterials 28(18):2876–2884

Le Douarin NM, Creuzet S (2011) Neural crest and vertebrate evolution. Biol Aujourdhui 205(2):87–94

Lee KJ, Nallathamby PD, Browning LM, Osgood CJ, Xu XN (2007) In vivo imaging of transport and biocompatibility of single silver nanoparticles in early development of zebrafish embryos. ACS Nano 1:133–143

Liu YX, Li W, Lao F, Liu Y, Wang LM, Bai R (2011) Intracellular dynamics of cationic and anionic polystyrene nanoparticles without direct interaction with mitotic spindle and chromosomes. Biomaterials 32:8291–8303

Lundqvist M, Stigler J, Elia G, Lynch I, Cedervall T et al (2008) Nanoparticle size and surface properties determine the protein corona with possible implications for biological impacts. Proc Natl Acad Sci USA 105:14265–14270

Lundqvist M, Stigler J, Cedervall T, Bergga T, Flanagan MB, Lynch I, Elia G, Dawson K (2011) The Evolution of the protein corona around nanoparticles: a test study. ACS Nano 5(9):7503–7509

Mahler GJ, Esch MB, Tako E, Southard TL, Archer SD, Glahn RP, Shuler ML (2012) Oral exposure to polystyrene nanoparticles affects iron absorption. Nat Nanotechnol 7:264–271. doi:10.1038/nnano

McCarthy J, Gong X, Nahirney D, Duszyk M, Radomski M (2011) Polystyrene nanoparticles activate ion transport in human airway epithelial cells. Int J Nanomed 6:1343–1356. doi:10.2147/IJN.S21145

Nam J, Won N, Bang J, Jin H, Park J, Jung S, Jung S, Park Y, Kim S (2013) Surface engineering of inorganic nanoparticles for imaging and therapy. Adv Drug Deliv Rev 65(5):622–648

Nieuwkoop PD, Faber J (1956) Normal table of *Xenopus laevis* (Daudin). North Holland Publishing Co, Amsterdam

Oslakovic C, Cedervall T, Linse S, Dahlbäck B (2012) Polystyrene nanoparticles affecting blood coagulation. Nanomedicine 8(6):981–986. doi:10.1016/j.nano.2011.12.001

Pompa PP, Vecchio G, Galeone A, Brunetti V, Sabella S, Maiorano G, Falqui A, Bertoni G, Cingolani R (2010) In vivo toxicity assessment of gold nanoparticles in *Drosophila melanogaster*. Nano Res 4(4):405–413

Sanfins E, Augustsson C, Dahlbäck B, Linse S, Cedervall T (2014) Size-dependent effects of nanoparticles on enzymes in the blood coagulation cascade. Nano Lett 14:4736–4744. doi:10.1021/nl501863u

Scales JB, Olson EN, Perry M (1990) Two distinct *Xenopus* genes with homology to *MyoD1* are expressed before somite formation in early embryogenesis. Mol Cell Biol 10(4):1516–1524

Scown TM, van Aerle R, Tyler CR (2010) Do engineered nanoparticles pose a significant threat to the aquatic environment? Crit Rev Toxicol 40:653–670

Smith JC, Price BM, Green JB, Weigel D, Herrmann BG (1991) Expression of a *Xenopus* homolog of *Brachyury* (T) is an immediate-early response to mesoderm induction. Cell 67(1):79–87

Spokony RF, Aoki Y, Saint-Germain N, Magner-Fink E, Saint-Jeannet J-P (2002) The transcription factor *Sox9* is required for cranial neural crest development in *Xenopus*. Development 129:421–432

Symens N, Walczak R, Demeester J, Mattaj I, De Smedt SC, Remaut K (2011) Nuclear inclusion of nontargeted and chromatin-targeted polystyrene beads and plasmid DNA containing nanoparticles. Mol Pharm 8(5):1757–1766. doi:10.1021/mp200120v

Takagi C, Sakamaki K, Morita H, Hara Y, Suzuki M, Kinoshita N, Ueno N (2013) Transgenic *Xenopus laevis* for live imaging in cell and developmental biology. Develop Growth Differ 55(4):422–433

Taylor MV, Gurdon JB, Hopwood ND, Towers N, Mohun TJ (1991) *Xenopus* embryos contain a somite-specific, MyoD-like protein that binds to a promoter site required for muscle actin expression. Genes Dev 5(7):1149–1160

Tian F, Razansky D, Estrada GG, Semmler-Behnke M, Beyerle A, Kreyling W, Ntziachristos V, Stoeger T (2009) Surface modification and size dependence in particle translocation during early embryonic development. Inhal Toxicol Suppl 1:92–96. doi:10.1080/08958370902942624

Tomlinson ML, Field RA, Wheeler GN (2005) *Xenopus* as a model organism in developmental chemical genetic screens. Mol BioSyst 1:223–228

Vaccaro MC, Cuccaro M, De Marco N, Campanella C (2006) Expression of p27BBP/eIF6 is highly modulated during *Xenopus laevis* embryogenesis. Mol Reprod Dev 73(4):482–490

Wick P, Malek A, Manser P, Meili D, Maeder-Althaus D, Diener L, Diener P-A, Zisch A, Krug HF, von Mandach U (2010) Barrier capacity of human placenta for nanosized materials. Environ Health Perspect 118:432–436

Xu R, Xiong B, Zhou R, Shen H, Yeung ES, He Y (2014) Pericellular matrix plays an active role in retention and cellular uptake of large-sized nanoparticles. Anal Bioanal Chem 406(20):5031–5037. doi:10.1007/s00216-014-7877-6

Yamamoto A, Honma R, Sumita M, Hanawa T (2004) Cytotoxicity evaluation of ceramic particles of different sizes and shapes. J Biomed Mat Res 68A:244–256

Yanagisawa KO, Fujimoto H, Urushihara H (1981) Effects of the *brachyury* (T) mutation on morphogenetic movement in the mouse embryo. Dev Biol 87(2):242–248